J. Phys.: Condens. Matter **11** (1999) 7143–7153. Printed in the UK PII: S0953-8984(99)02672-7

The density of states and first spectral moments of a quasiperiodic lattice

Gerardo G Naumis

Instituto de Física, Universidad Nacional Autónoma de México (UNAM), Apartado Postal 20-364, 01000, Distrito Federal, Mexico

Received 12 March 1999, in final form 13 July 1999

Abstract. The density of states of a tight-binding Hamiltonian on a two-dimensional quasiperiodic lattice (the Penrose tiling) is studied in terms of the first spectral moments. This approach shows that there is a tendency for a depletion of the local density of states at certain sites of the lattice, and a progressive localization of states at the centre of the spectrum. The effect of different kinds of phason flips in the first moments is also studied.

1. Introduction

Since the discovery of quasicrystals in 1984 [1], it has been clear that they are a new type of structure with a peculiar kind of order: despite lacking translational periodic order, the positions of the atoms are precisely determined. In view of this new class of long-range order, interesting physical properties of these materials were expected.

In the last few years, with the advent of high-quality quasicrystalline samples, there has been found clear evidence that quasicrystals have singular electronic properties. They have abnormally high electrical resistivity [2], and the conductivity is improved by the introduction of impurities and structural defects and by increasing the temperature [3]. Also, the appearance of a pseudo-gap at the Fermi level seems to be a universal feature of quasicrystals [4]. This is a very important fact, because it leads to a Hume-Rothery mechanism for the structure stabilization [5, 6].

Some of these questions will be cleared up if we achieve a full understanding of QP Hamiltonians [7]. However, only for one-dimensional lattices are the nature of the spectrum and the localization properties of the wave-function well understood. For these systems, the spectrum is singular continuous [8, 9], and the eigenstates are critical; these are non-normalizable self-similar wave-functions with a power-law decay of the amplitude [7, 10]. For two and three dimensions, the nature of the spectrum is still an open question, although there have been a lot of numerical calculations made with the aim of elucidating this question [11–13].

In two and three dimensions, studies of the electronic structure in QP lattices are usually based on a tight-binding model. For such QP lattices, the Penrose tiling (PT) has been the most popular system, since it is the lowest-dimensional model with topological quasiperiodicity [7]. This QP topology of the PT makes it very different from one-dimensional lattices, since it contains new mechanisms that do not appear in one-dimensional lattices, like frustration of wave-functions in odd rings, which can affect their localization properties at different energies [13].

0953-8984/99/377143+11$30.00

In the PT, two kinds of models can be defined: the vertex model, where the atomic orbitals are placed on the vertices of the tiles that define the lattice, and the centre model, where the orbitals are at the centres of the tiles. In both cases, an electron can only hop between neighbouring orbitals. This leads to the following Hamiltonian:

$$H = \sum_{i,j} |i\rangle\langle j|. \tag{1}$$

For these two models, the first numerical calculations for a tight-binding Hamiltonian showed that three kinds of wave-functions coexist: extended, localized and critical [11]. It was further shown numerically that the decay of the wave-functions follows a power law with a multi-fractal structure [7, 12]. This decay is due to the competition between two mechanisms: on one hand, Conway's theorem tends to delocalize states since it causes resonances between equivalent local configurations [7] (Conway's theorem states that the distance between two identical local configuration of radius R in a PT is at most $4R$). On the other hand, the dense Bragg spots in the reciprocal space of a QC imply localization, since an unperturbed Bloch function will be hybridized with a number of wave-functions with various momenta owing to the potential scattering [7]. More recently, this scenario was confirmed at least for some states by Repetowicz *et al* [14], who found exact critical states in the PT for certain energies by following previous work of Sutherland [15]. However, it is also known that there are strictly localized states, since they have amplitude in certain regions of the tiling, and zero outside. These states are called *confined* [16]; they are infinitely degenerate and correspond to particular values of the energy. These states occur as a consequence of the local topology of the lattice [17], and are separated from the rest of the spectrum by an energy gap [13, 16]. Observe that one must be careful about the nature of these states, since due to their degeneracy, any linear combination of them is also an eigenstate, and these linear combinations may be extended, although they are called confined in the literature [16].

In the vertex problem, this gap and the confined states appear at the centre of the spectrum, $E = 0$, which also serves as a symmetry axis for the electronic spectrum (this symmetry is due to the bipartite property of the lattice, i.e., it can be subdivided into two alternating sublattices, say A and B, and an electron can only hop from an A site onto a B site or back). An interesting point about the whole structure of this spectrum is the fact that the states tend to be more localized at the centre of the spectrum [12, 13, 18], in contrast to Anderson localization, where the states are localized at the tails of the band edges. Furthermore, this localization produces a strong multi-fractal behaviour on changing the energy from the band edges to the band centre [12]. As was observed numerically [13], the tendency is for the states to localize in a similar way to confined states, i.e., the sites with a high coordination number have a vanishing LDOS as we approach $E = 0$ [13].

Another interesting question is the effect of disorder on the electronic properties of a quasiperiodic lattice. In particular, quasicrystals present defects that are local rearrangments of tilings. These defects are called phasons, since they are extra hydrodynamic modes which appear as a consequence of a broken symmetry in the higher-dimensional space that is associated with a quasicrystal. In one dimension, it was found that phasons can change in a substantial way the spectrum of quasiperiodic systems, due to the self-similar structure of the gaps [19, 20]. Furthermore, phasons can change the energy-level-spacing distribution by diminishing the tendency of clustering observed in one-dimensional quasicrystals, since localized states appear over all of the original self-similar spectral gaps [20]. For two-dimensional tilings, a similar global change of the level statistics with phason disorder has been reported [21]. However, there are new results which suggest that this was an artifact of a hidden symmetry, because the appropriate level statistics for such two-dimensional systems is universal, and corresponds to the Gaussian orthogonal ensemble of random-matrix

theory [22, 23]. For the PT, a numerical study showed that phasons enhance localization at some energies, and the conductance decreases, while they increase conductance at the original energy gaps [24]. Schwabe, Kasner and Böttger considered the effect of each of the seven possible phason flips in the PT [25]. They found a localized state in the defect region, and a smoothing out of the DOS with very strong fluctuations of the conductance in most of the energy regions, but the strength of this effect depends strongly on the type of flips [25]. As we will show, these differences are due to the local topology of each kind of phason.

The aim of this article is to show that the depletion of the LDOS at the high-coordination sites, and the tendency for the wave-function to avoid sites of high coordination numbers, can be explained in terms of the local topology of the PT. To prove this point, in section 2 we evaluate the first spectral moments of a PT using the Cyrot-Lackmann theorem [26], which relates the LDOS to the topology of the local atomic environment. In section 3 we study the effect of phason disorder on this tendency for depletion of the LDOS, and finally, in section 4 the conclusions are given.

2. Spectral moments of a Penrose tiling

In this section, we investigate the spectral moments of the vertex model in a PT, and the information that they give about the spectrum. We start by defining the moment of order n for a tight-binding Hamiltonian [27]:

$$\mu_i^{(n)} = \int_{-\infty}^{\infty} (E - H_{ii})^n \rho_i(E)\, \mathrm{d}E \tag{2}$$

where $\rho_i(E)$ is the local density of states at site i. The moment $\mu_i^{(0)}$ is always one, owing to the normalization condition of the basis ($\langle i|i\rangle = 1$). The first moment, $\mu_i^{(1)}$, is the centre of gravity of the LDOS, which in this case is the centre of the spectrum relative to H_{ii}. In the vertex problem for the PT, all the self-energies are set to zero ($H_{ii} = 0$), and thus the centre of gravity of the spectrum is $E = 0$. The next moment, $\mu_i^{(2)}$, is a measure of the 'moment of inertia' of the LDOS with the centre of gravity. The third moment, $\mu_i^{(3)}$, measures the skewness about the centre of gravity. The fourth moment measures the tendency for depletion of the LDOS at the middle of the spectrum [27]. A low value of the normalized fourth moment, $\mu_i^{(4)}/(\mu_i^{(2)})^2$, corresponds to two well separated peaks in the LDOS; this behaviour is called bimodal, whereas a large value corresponds to a central peak or unimodal behaviour [27]. In fact, a precise criterion can be given to discriminate between unimodal and bimodal forms of the LDOS. This criterion is as follows. We first calculate the dimensionless parameter s_i,

$$s_i = \frac{\mu_i^{(4)}\mu_i^{(2)} - (\mu_i^{(2)})^3 - (\mu_i^{(3)})^2}{(\mu_i^{(2)})^3}. \tag{3}$$

If $s \geqslant 1$ we have unimodal behaviour, while for $s < 1$ we have bimodal behaviour [27]. This parameter s is the one that we are going to obtain for the PT, in order to discern the tendency for a gap opening at the middle of the spectrum (for example, a square lattice, which is unimodal with a Van Hove singularity at $E = 0$, gives $s = 1.25$, while a honeycomb lattice, which has a vanishing LDOS at $E = 0$, gives $s = 0.67$).

In principle, one can express the LDOS using the moments of the spectrum. However, in practice one needs to know all the moments up to infinity [28], since the corresponding expression for obtaining the LDOS converges very slowly. Due to this, in this article we will find the second and fourth moments because they are the ones that give most of the information about the overall shape of the spectrum.

A useful way to obtain the firsts moments needed in equation (3) is to use the Cyrot-Lackmann theorem, which states that the moment of order n is given by [26]

$$\mu_i^{(n)} = \langle i|H^n|i\rangle. \tag{4}$$

which is the sum of all possible paths of length-n hops, starting and ending at site i.

The second moment is always equal to the local coordination at the site (Z_i):

$$\mu_i^{(2)} = Z_i. \tag{5}$$

In the PT, Z_i can be 3, 4, 5, 6 and 7, depending on the type of vertex; these are labelled as Q, D, K, S_5, J, S, S_6 and S_3 [29], as shown in figure 1. These different types of vertices that appear in the PT are also displayed in table 1 (denoted by γ), with their respective coordination numbers and frequencies ($P(\gamma)$) in the lattice. From this table, it is clear that the sites with lower coordination Q and D have narrower LDOS than those with higher coordination, S_3 and S_4, as was observed in numerical calculations [13]. Using the LDOS, we can also obtain the complete density of states (DOS) since it corresponds to the sum of the LDOS at all sites. Thus, the second moment of the DOS is the sum of all the second moments of the LDOS:

$$\mu^{(2)} = \sum_i \mu_i^{(2)}. \tag{6}$$

For quasiperiodic lattices, the sum that appears above can be substituted for with a sum over the different kind of sites, multiplied by the probability of occurrence of each kind of site, which leads to

$$\mu^{(2)} = \sum_\gamma P(\gamma) Z_\gamma = \langle Z\rangle \tag{7}$$

where $\langle Z\rangle$ is the *average coordination number* of the lattice. In a PT, $\langle Z\rangle$ is 4. This number is a good estimate of the bandwidth, which is nearly 4.23 in the PT [16] (a much better estimate [13] is the square root of $\langle Z^2\rangle$).

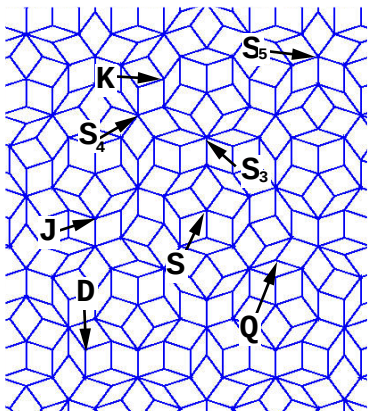

Figure 1. Different vertex configurations that appear in the PT, with their corresponding labels.

The third moment is given by the number of all closed paths of length-3 hops. However, since the lattice is composed of rhombi, with interaction only along their edges, there are no paths of this type. Thus, $\mu^{(3)}$ is zero. This is always true for any odd moment, and as a result the whole spectrum is symmetric around $E = 0$. Observe that this fact is related to the bipartite nature of the lattice, since a lattice formed by rhombi is always bipartite.

To obtain the fourth moment, we observe that at a typical site of the PT, there are three kinds of closed paths of fourth hops, as shown in figure 2.

Table 1. Parameter s.

Vertex (γ)	Z_γ	$P(\gamma)$	Neighbours (c)	$P(\gamma, c)$	$N_{TSP}(\gamma, c)$	$\mu^{(4)}_{\gamma,c}$	$\langle Z_{\gamma,c}\rangle$	$s_{\gamma,c}$	$\langle s_\gamma\rangle$
Q	3	$1/\tau^4$[a]	S_3, 2J	$1/\tau^2$	14	29	5.67	2.22	
			S_4, 2J	$1/\tau^3$	13	28	5.33	2.11	2.20
D	3	$1/\tau^2$	S, S_3, J	$2/\tau^4$	14	29	5.66	2.22	2.10
			S, 2J	$1/\tau^3$	12	27	5.00	2.0	
			K, S_4, J	$2/\tau^5$	12	27	5.00	2.0	
			K, S_3, J	$2/\tau^4$	13	28	5.33	2.11	
K	4	$1/\tau^5$	2D, 2J	1	12	36	4.00	1.25	1.25
S_5	5	$(3-\tau)/5\tau^6$	5J	1	20	55	5.00	1.20	1.20
J	5	$1/\tau^3$	2K, 2D, S_3	$1/\tau^3$	16	51	4.20	1.04	0.95
			Q, K, 2D, S_4	$2/\tau^4$	14	49	3.80	0.52	
			2Q, 2D, S_4	$1/\tau^4$	13	48	3.60	0.48	
			2Q, 2D, S_5	$5/\tau^3(1+\tau^2)$	12	47	3.40	0.44	
S	5	$(2+\tau)/5\tau^6$	5D	1	10	45	3.00	0.80	0.80
S_4	6	$1/\tau^7$	Q, 2D, 3J	1	18	66	4.00	0.83	0.83
S_3	7	$1/\tau^6$	2Q, 4D, J	1	16	79	3.28	0.61	0.61

[a] τ is the golden section $(1+\sqrt{5})/2$.

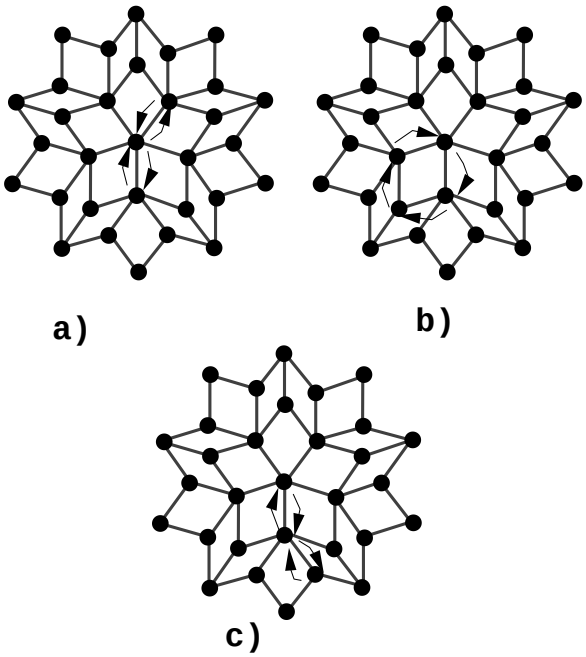

Figure 2. The three different kinds of paths that contribute to the fourth moment: (a) revisiting paths (RVP), (b) loop paths (LP) and (c) paths with three sites, non-revisiting with no loops (TSP).

In the first kind (figure 2(a)), the electron starts at the vertex γ, and hops to one of its neighbours j, and again hops to the original vertex. Then it can hop again to a neighbouring

site. We will call this type revisiting paths (RVP). The number of these paths is only Z_γ^2, because the first and third jumps can be made in Z_γ ways, while the second and fourth are determined by the condition of revisiting the original site.

The second kind of paths are those that follow the edges of the rhombi that have the vertex γ as one corner (figure 2(b)). We call these paths loops (LP). The number of these paths is $2Z_\gamma$, because there are Z_γ rhombi that have γ as a corner, and there are two senses of circulation in each rhombus.

Finally, the third contribution comes from paths that visit once the second neighbours of the original site but do not form a loop (figure 2(c)). We will refer to these paths as three-site non-revisiting with no loops (TSP). The number of these paths (N_{TSP}) depends on the distribution and coordination of the neighbours of the site. Observe that given a certain kind of vertex γ, there are different configurations of neighbours, each of them with a different frequency. If we call a given configuration of site neighbours c, the number of TS paths ($N_{TSP}(\gamma, c)$) is

$$N_{TSP}(\gamma, c) = \sum_{\sigma=1}^{Z_\gamma} (Z_\sigma - 1) \tag{8}$$

where Z_σ is the coordination of each of the Z_γ neighbours. For example, a three-coordinated Q site has two kinds of surrounding configurations. The first has two J sites and one S_4, which gives 13 TSP paths. The other has two J sites and one S_3, to give 14 paths. The first configuration occurs with a frequency $(1/\tau^3) = 0.23$ around a Q site, while the other has a frequency $(1/\tau^4) = 0.76$.

The fourth moment in a site of type γ, with a surrounding configuration of sites c, is given by the sum of the three kinds of paths (RVP, LP and TSP):

$$\mu_{\gamma,c}^{(4)} = Z_\gamma^2 + 2Z_\gamma + \sum_{\sigma=1}^{Z_\gamma} (Z_\sigma - 1). \tag{9}$$

Finally, the parameter $s_{\gamma,c}$ is obtained when equation (9) and equation (5) are substituted into equation (3):

$$s_{\gamma,c} = \frac{1}{Z_\gamma}\left(1 + \frac{1}{Z_\gamma}\sum_{\sigma=1}^{Z_\gamma} Z_\sigma\right) = \frac{1}{Z_\gamma} + \frac{\langle Z_{\gamma,c}\rangle}{Z_\gamma} \tag{10}$$

where we have defined $\langle Z_{\gamma,c}\rangle$ as the average coordination number, for a given configuration c, of the neighbours of γ:

$$\langle Z_{\gamma,c}\rangle = \frac{1}{Z_\gamma}\sum_{\sigma=1}^{Z_\gamma} Z_\sigma. \tag{11}$$

Equation (11) shows that $s_{\gamma,c}$ has two contributions: one is proportional to the inverse of Z_γ, and the other is the ratio between the average coordination number of the neighbours and the coordination of the given site.

For comparison proposes, we can define an average parameter $\langle s_\gamma\rangle$ for each kind of site, by taking the average over s_γ for all the possible neighbour configurations:

$$\langle s_\gamma\rangle = \sum_c P(\gamma, c) s_{\gamma,c} \tag{12}$$

where $P(\gamma, c)$ is the probability of observing the configuration c of neighbours of γ.

In table 1 we show, in the first three columns, the different kinds of vertices that appear in the PT with their corresponding coordination and frequencies. The following columns contain

the corresponding allowed configurations of neighbouring vertices for each kind of vertex, and their frequencies. We also include the number of TSP ($N_{TSP}(\gamma, c)$), the fourth moment and the average coordination number for each configuration of neighbours. Finally, using equation (10), the parameter $s_{\gamma,c}$ can be calculated for each configuration, and the average $\langle s \rangle$ is also shown.

From table 1, we observe that the LDOS is unimodal for sites of type Q, D, K and S_5, while for J, S, S_4 and S_3 sites it is bimodal. As is clearly seen, sites with higher coordination numbers have a bimodal character, i.e., there is a tendency for a depletion of the LDOS at the middle of the spectrum.

This fact can be explained if we observe that in equation (10), the condition for the depletion of the LDOS ($s < 1$) can be recast as

$$Z_\gamma \geqslant \langle Z_{\gamma,c} \rangle + 1. \tag{13}$$

In a PT, the last condition holds for higher coordination numbers because these sites are always surrounded by sites of lower coordination. For example, from table 1, we can see that a site S_3 always has six vertices with coordination 3, and one vertex with coordination 6 as neighbours, to give an average of 3.28. The reverse is true for lower-coordination sites, since they are surrounded by sites with higher coordination numbers. Thus, sites of lower coordination have a unimodal LDOS. This fact is a consequence of the local deviations of the statistics of vertices, which has 4 as the average coordination number. Furthermore, if we make the rough assumption that $\langle Z_{\gamma,c} \rangle$ is nearly equal to the average coordination number of the whole lattice, 4, then from equation (13) we get that $Z_\gamma > 5$, as is observed for the lattice. Sites with coordination 5 are the exception. An S_5 site is unimodal because it is surrounded only by sites of coordination 5, and a J site with 2K, 2D and S_3 as neighbours is also unimodal. Other sites with coordination 5 are bimodal.

An interesting observation is that in the PT, all non-three-site vertices are connected in lines (called strings) which divide the complete lattices into independent parts [16]. These parts contain only three-edge vertices (notice that these strings can be closed lines, and thus they are not the same regions that define the worms [30]). These strings are the same as those that confine inside them all eigenstates at $E = 0$, where it is known that the amplitude of the wave-function is always zero in the string (except at the S_5 and J sites with 2K, 2D and S_3 as neighbours, which are the same exceptions as we found [31]). The present results suggest that the wave-functions at the centre of the spectrum have a similar distribution of amplitudes to those at $E = 0$, since the LDOS is given by

$$\rho_i(E) = \sum_\alpha \delta(E - E_\alpha) \| \langle i | \alpha \rangle \|^2 \tag{14}$$

where E_α is an eigenvalue, and thus we expect a reduction of the amplitude for sites where $\rho_i(E)$ is small. Notice that the other factor $\delta(E - E_\alpha)$ is not responsible for the lowering of the LDOS, since there are states close to $E = 0$, as is indicated by the fact that the LDOS is high for lower-coordination sites. This analysis is consistent with the observed tendency for a strong localization [12], and the reduction in the participation ratio of the wave-function for high coordination numbers at the centre of the spectrum [13].

It is important to remark that confined states at $E = 0$ do not make any contribution to the moments of the spectrum, since they are at the centre of gravity. However, they have an indirect impact on the LDOS, since they can reduce the relative weight of the states with $E \neq 0$. In the case of sites with coordination different from 3, there is no impact, since those sites are forbidden for states with $E = 0$. The only allowed sites for states at $E = 0$ are three-coordinated sites. We can exclude these states in order to obtain the overall shape of the LDOS, if we assume that the fraction of states at $E = 0$ is known. For doing this, we define

a new LDOS at three-coordinated sites ($\rho_i^*(E)$) which excludes the delta function at $E = 0$. This LDOS is a scaled version of the original LDOS, $\rho_i^*(E) = \lambda\rho_i(E)$, where λ is equal to $(1 - f_0)^{-1}$, and f_0 is the fraction of states at $E = 0$. The new LDOS satisfies the following condition:

$$2\lim_{\epsilon\to 0}\int_{-\infty}^{\epsilon}\rho_i^*(E)\,\mathrm{d}E = 1. \tag{15}$$

The moments of $\rho_i^*(E)$ are also a scaled version of the original moments, i.e., $\mu_i^{*(n)} = \lambda\mu_i^{(n)}$. The corresponding parameter s^* of $\rho_i^*(E)$ is given by

$$s^* = \frac{s+1}{\lambda} - 1 = (1 - f_0)(s + 1) - 1. \tag{16}$$

Since f_0 is nearly $1/10$ in the PT [13], we obtain that the unimodality of three-coordinated sites is reduced when we exclude states at $E = 0$.

3. Spectral moments of the tiling with phason flips

In a PT, a phason flip consists in a rearrangment of three tiles, and can be made only at a Q or D vertex, as shown in figure 3. According to table 1, there are two different configurations of first neighbours for a Q vertex and four for D. This gives six different kind of flips. However, in the hexagon that contains a Q vertex, one of the vertices can be an S site or an S_4. This fact leads to the seven different types of flips considered by Schwabe *et al*. In order to label all the possible flips, we followed the scheme of Schwabe *et al*, as shown in figure 3. The labels can also be found in table 2, where (a), (b), (c), (d), (e), (f) and (g) denote the possible neighbouring configurations of a Q and D vertex. The effect on the first moments of the LDOS of the phason flips can be obtained by counting the new number of paths produced by each kind of flip. The sites affected by these changes are the Q or D sites where phasons

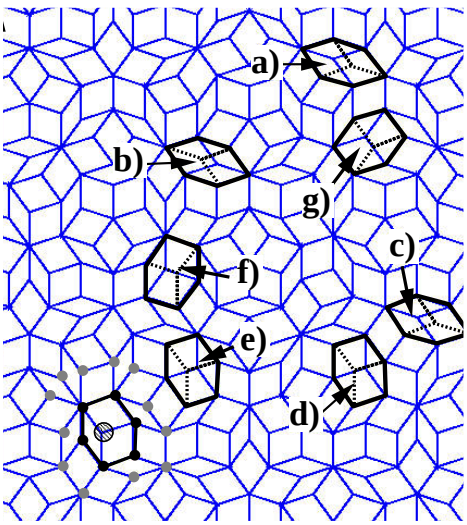

Figure 3. The seven kinds of flip that can be made in a PT, with their corresponding labels. The hexagons that surround the phason flips are shown with bold lines, and the new configurations that appear after the flip are shown with dotted lines. In the bottom left corner of the figure, the circles correspond to the sites that can change their second or/and fourth moment after a phason flip is applied in their neighbourhood.

Table 2. Phason flips.

Vertex	Flip label	Neighbours	$\langle Z'_{\gamma,c}\rangle$	s'
Q	(a)	S_3, 2J	4.67	1.89
	(b)	S_3, 2J	5.0	2.0
	(c)	S_4, 2J	4.67	1.89
D	(d)	S, 2J	4.33	1.78
	(e)	S, S_3, J	4.0	1.67
	(f)	K, S_3, J	4.67	1.89
	(g)	K, S_4, J	4.67	1.89

are made, the sites that form the hexagon that contains the three-coordinated sites and the sites that are first neighbours of the hexagon. These three kinds of vertices that are in the neighbourhood of a phason flip are shown with dashed, black and grey circles in figure 3, respectively.

First we will consider the effect on the Q or D vertex where the phason is made. In this case, after a flip is performed, the first neighbours of a Q or D change, but since the coordination number remains constant, the second moment is the same as before. However, the new average coordination of the neighbours $\langle Z'_{\gamma,c}\rangle$ is decreased, and thus the unimodality of the spectrum is also slightly decreased, as can be seen in the corresponding new parameter s' that appears in the last column of table 2. A comparison with table 1 shows that phasons of type (a) and (e) have a greater impact on the LDOS than other kinds.

The sites that are in the hexagon that surround a flipped vertex change their second and fourth moments. In this hexagon, there are three sites that change their coordination from Z_i to $Z_i - 1$ when the flip is produced, while there are three others that change from Z_i to $Z_i + 1$. The new fourth moment is

$$\mu^{(4)}_{i,c} = (Z_i \pm 1)^2 + 2(Z_i \pm 1) + \sum_{\sigma=1}^{Z_i}(Z_\sigma - 1) \tag{17}$$

where the upper sign corresponds to the case when the coordination is raised, while the other holds for the opposite case. Here Z_σ is the coordination of the neighbours of site i in the original PT. The new parameter s' is given by

$$s' = \frac{2}{Z_i \pm 1} + \frac{Z_i}{(Z_i \pm 1)^2}(\langle Z_\sigma\rangle - 1). \tag{18}$$

To elucidate whether this parameter is bigger or smaller than the original one, we perform an expansion of $(1 + (1/Z_i))^{-1}$, which gives up to first order

$$s' \approx s \mp 2\left(\frac{1}{Z_i} + \frac{(\langle Z_\sigma\rangle - 1)}{Z_i^2}\right). \tag{19}$$

From here, it is clear that sites which reduce (raise) their coordination with the phason flip increase (decrease) their unimodality. Observe that this result does not depend on the kind of phason flip.

The sites that have as neighbours the sites in the hexagon (grey circles in figure 3) are also affected by the flip in their fourth moment but not in the second. In this case, the number of four-hop paths is reduced only by one if the site is neighbour of a site that was connected to the Q or D site of the flip, while it is increased by one in any other case. Thus, in the first case the unimodality is decreased, while in the second it is raised.

From the above results, we can say that at the level of the second and fourth moments, each type of phason flip changes the DOS in a different way, and the difference comes from the changes in the average coordination number around the Q or D site where the phason is made.

4. Conclusions

In this work, we calculated the first moments of a Penrose tiling using the Cyrot-Lackmann theorem. These moments were used to investigate the LDOS and the localization of states. The results show that for sites with high coordination numbers, there is a tendency for a depletion of the LDOS at the middle of the spectrum. This is due to the local fluctuations of the coordination number. Furthermore, near the centre of the spectrum, states follow a localization pattern similar to those for states at $E = 0$, with a reduction of the amplitude at sites of high coordination. This phenomenon can be attributed to the topology of the lattice, where sites of high coordination are surrounded by sites with lower coordination numbers. These high-coordination regions form strings which isolate low-coordination-number sites. Observe that this phenomenon is very similar to what happens in the split-band regimen of a random binary alloy, in which sites with high self-energy act as barriers to the wave-function, and tend to localize inside regions of low self-energy [32]. For the PT, the coordination number acts as a self-energy. In fact, the spectrum of the binary alloy in the split-band regimen for a square lattice has many properties that are observed in the PT, like confined states and a gap [32] at $E = 0$. This is why the spectrum of the PT can be compared much better with the square-lattice random alloy [33] than a pure square lattice, as was proposed by Choy [34].

In this paper, it was also shown that phason disorder changes the LDOS in different ways, depending on the kind of flips, since the average coordination number of neighbours around a phason is changed.

The present approach suggests the study of much more realistic models in order to evaluate the cohesive energy of quasicrystals. Some of this work is currently in progress.

Acknowledgments

I would like to thank Professors R J Elliot, M F Thorpe, Chumin Wang, E Maciá and R A Barrio for useful discussions, and an anonymous referee for suggestions. This work was supported by CONACyT through grant 25237-E, and DGAPA UNAM project IN119698.

References

[1] Shechtman D, Blech I, Gratias D and Cahn J W 1984 *Phys. Rev. Lett.* **53** 1951
[2] Pierce F S, Poon S J and Guo Q 1993 *Science* **261** 737
[3] Mayou D, Berger C, Cyrot-Lackmann F, Klein T and Lanco P 1993 *Phys. Rev. Lett.* **70** 3915
[4] Poon S J 1992 *Adv. Phys.* **4** 303
[5] Friedel J 1998 *Helv. Phys. Acta* **61** 538
[6] Belin E, Dankhazi Z, Sadoc A, Dubois J M and Calvayrac J M 1994 *Europhys. Lett.* **26** 677
[7] Tsunetsugu H, Fujiwara T, Ueda K and Tokihiro T 1991 *Phys. Rev.* B **43** 8879
[8] Sütő A 1989 *J. Stat. Phys.* **56** 525
[9] Kohmoto M, Kadanoff L P and Tang Chao 1983 *Phys. Rev. Lett.* **50** 1870
[10] Maciá E and Domínguez-Adame F 1996 *Phys. Rev. Lett.* **76** 2957
[11] Ma P and Liu Y 1989 *Phys. Rev.* B **39** 9904
[12] Rieth T and Schreiber M 1998 *J. Phys.: Condens. Matter* **10** 783
[13] Naumis G G, Barrio R A and Wang Chumin 1994 *Phys. Rev.* B **50** 9834
[14] Repetowicz P, Grimm U and Schreiber M 1998 *Phys. Rev.* B **58** 13 482

[15] Sutherland B 1986 *Phys. Rev.* B **34** 3904
[16] Kohmoto M and Sutherland B 1986 *Phys. Rev. Lett.* **56** 2740
[17] Rieth T and Schreiber M 1995 *Phys. Rev.* B **51** 15 827
[18] Rieth T and Schreiber M 1995 *Proc. 5th. Int. Conf. on Quasicrystals* ed Ch Janot and R Mosseri (Singapore: World Scientific) p 514
[19] Naumis G G and Aragón J L 1996 *Phys. Rev.* B **54** 15 079
[20] Naumis G G and Aragón J L 1998 *Phys. Lett.* A **244** 133
[21] Piéchon F and Jagannathan A 1995 *Phys. Rev.* B **51** 179
[22] Zhong J X, Grimm U, Römmer R A and Schreiber M 1998 *Phys. Rev. Lett.* **80** 3996
[23] Grimm U, Romer R A and Schliecker G 1998 *Ann. Phys., Lpz.* **7** 389
[24] Yamamoto S and Fujiwara T 1994 *Mater. Sci. Eng.* A **181+182** 726
[25] Schwabe H, Kasner G and Böttger H 1999 *Phys. Rev.* B **59** 861
[26] Cyrot-Lackmann F 1968 *J. Phys. Chem. Solids* **29** 1235
[27] Sutton A P 1993 *Electronic Structure of Materials* (Oxford: Clarendon) p 66
[28] Ziman J M 1979 *Models of Disorder* (Cambridge: Cambridge University Press)
[29] de Bruijn N G 1981 *Math. Proc.* A **84** 39
[30] Janot C 1992 *Quasicrystals: a Primer* (Oxford: Oxford University Press) p 343
[31] Arai M, Tokihiro T, Fujiwara T and Kohmoto M 1998 *Phys. Rev.* B **38** 1621
[32] Kirkpatrick S and Eggarter T P 1972 *Phys. Rev.* B **6** 3598
[33] Naumis G, Barrio R A and Wang Chumin 1995 *Proc. 5th. Int. Conf. on Quasicrystals* ed Ch Janot and R Mosseri (Singapore: World Scientific) p 514
[34] Choy T C 1985 *Phys. Rev. Lett.* **55** 2915